G protein-dependent presynaptic inhibition mediated by AMPA receptors at the calyx of Held

Hideki Takago*†‡, Yukihiro Nakamura*‡, and Tomoyuki Takahashi*§

*Department of Neurophysiology, University of Tokyo Graduate School of Medicine, Hongo, Bunkyo, Tokyo 113-0033, Japan; and †Department of Otolaryngology, Tokyo Medical and Dental University Graduate School, Yushima, Bunkyo, Tokyo 113-8519, Japan

Edited by Roger A. Nicoll, University of California, San Francisco, CA, and approved April 1, 2005 (received for review November 16, 2004)

The α-amino-3-5-methyl-4-isoxazolepropionic acid receptor (AMPAR) is an ionotropic receptor mediating excitatory synaptic transmission, but it can also interact with intracellular messengers. Here we report that, at the calyx of Held in the rat auditory brainstem, activation of AMPARs induced inward currents in the nerve terminal and inhibited presynaptic Ca^{2+} currents (I_{pCa}), thereby attenuating glutamatergic synaptic transmission. The AMPAR-mediated I_{pCa} inhibition was disinhibited by a strong depolarizing pulse and occluded by the nonhydrolyzable GTP analog GTPγS loaded into the terminal. We conclude that functional AMPARs are expressed at the calyx of Held nerve terminal and that their activation inhibits voltage-gated Ca^{2+} channels by an interaction with heterotrimeric GTP-binding proteins (G proteins). Thus, at a central glutamatergic synapse, presynaptic AMPARs have a metabotropic nature and regulate transmitter release by means of G proteins.

calcium channel | excitatory postsynaptic current | synapse | glutamate

Postsynaptic α-amino-3-5-methyl-4-isoxazolepropionic acid receptors (AMPARs) mediate glutamatergic synaptic transmission (1, 2). In addition to their well established ionotropic nature, AMPARs are reported to have a metabotropic nature, interacting with the G protein Gi (3) or the tyrosine kinase Lyn (4). AMPAR immunoreactivity has been demonstrated at nerve terminals (5, 6). At the primary sensory nerve terminal, AMPARs regulate transmitter release by means of an ionotropic action (7), whereas a metabotropic action of AMPARs is proposed to underlie presynaptic inhibition at cerebellar inhibitory synapses (8).

In the mammalian CNS, nerve terminals at most synapses are too small to make detailed electrophysiological analysis. However, at the calyx of Held visualized in slices of rodent brainstem, whole-cell patch-clamp recordings can be made directly from a giant nerve terminal (9), and various molecules can be applied into the terminal through patch pipettes (10, 11). Using this preparation, we demonstrate here that functional AMPARs are expressed in the calyceal nerve terminal and inhibit voltage-gated Ca^{2+} currents through a coupling with heterotrimeric G proteins.

Methods

Preparations and Solutions. All experiments were performed in accordance with the guidelines of the Physiological Society of Japan. Wistar rats (7–8 days old) were decapitated under halothane anesthesia, and the brain was quickly removed. Transverse brainstem slices (175–250 μm in thickness) containing the medial nucleus of the trapezoid body (MNTB) were cut by using a tissue slicer (ZERO-1, Dosaka, Kyoto, Japan) as described in ref. 12. Slices were incubated at 37°C for 30 min and subsequently maintained at room temperature in artificial cerebrospinal fluid (aCSF) containing 125 mM NaCl, 2.5 mM KCl, 26 mM $NaHCO_3$, 1.25 mM NaH_2PO_4, 2 mM $CaCl_2$, 1 mM $MgCl_2$, 10 mM glucose, 3 mM myo-inositol, 2 mM sodium pyruvate, and 0.5 mM ascorbic acid, pH 7.4, when bubbled with 95% O_2 and 5% CO_2. MNTB neurons and calyces were visualized with a ×60 water immersion objective lens (Olympus, Tokyo) attached to an upright microscope (Axioskop, Zeiss). For recording excitatory postsynaptic currents (EPSCs), the aCSF routinely contained bicuculline methiodide (10 μM, Sigma) and strychnine hydrochloride (0.5 μM, Sigma) to block inhibitory synaptic responses. The patch pipette solution for postsynaptic recording contained 110 mM CsF, 30 mM CsCl, 10 mM Hepes, 5 mM EGTA, and 1 mM $MgCl_2$ (295–305 milliosmolar, pH 7.3, adjusted with CsOH). *N*-(2,6-diethylphenylcarbamoylmethyl)-triethyl-ammonium chloride (QX314, 5 mM, Alomone Labs, Jerusalem) was also included in the pipette solution to block action potential generation. The pipette solution for recording calcium currents from calyceal terminals contained 110 mM CsCl, 10 mM tetraethylammonium chloride (TEACl), 40 mM Hepes, 0.5 mM EGTA, 1 mM $MgCl_2$, 12 mM Na_2 phosphocreatine, 2 mM ATP-Mg, and 0.5 mM GTP-Na (295–305 milliosmolar, pH 7.3 adjusted with CsOH). The pipette solution for recording presynaptic barium currents (I_{pBa}) contained 95 mM CsCl, 10 mM TEACl, 40 mM Hepes, 10 mM EGTA, 6 mM $CaCl_2$, 1 mM $MgCl_2$, 12 mM Na_2 phosphocreatine, 2 mM ATP-Mg, and 0.5 mM GTP-Na (295–305 milliosmolar, pH 7.3 adjusted with CsOH). The pipette solution for recording presynaptic potassium currents (I_{pK}) and current-clamp recording contained 97.5 mM potassium gluconate, 32.5 mM KCl, 10 mM Hepes, 5 mM EGTA, 1 mM $MgCl_2$, 12 mM Na_2 phosphocreatine, 2 mM ATP-Mg, and 0.5 mM GTP-Na (295–305 milliosmolar, pH 7.3, adjusted with KOH). Tetrodotoxin (1 μM) (Wako Pure Chemical, Osaka, Japan) was added to aCSF in the presynaptic recordings, and TEACl (10 mM, equimolar replacement of NaCl) was also added for recording calcium or barium currents.

Recording and Analysis. Whole-cell patch-clamp recordings were made from MNTB principal neurons or presynaptic calyceal nerve terminals. EPSCs were evoked every 20 s by extracellular stimulation of presynaptic axons using a bipolar tungsten electrode positioned halfway between the midline and the MNTB. For recording presynaptic Ca^{2+} currents (I_{pCa}), I_{pBa}, and I_{pK}, calyces were voltage-clamped at a holding potential of −80 mV, and depolarizing voltage steps were applied every 10–20 s. The current amplitude was measured 2–3 ms after the onset of the depolarizing pulse. The electrode resistance was 2–4 MΩ for postsynaptic recordings and 5–8 MΩ for presynaptic recordings. The access resistance of postsynaptic recordings was 7–21 MΩ and was not compensated for. The presynaptic access resistance was 7–20 MΩ and was compensated by up to 80%. Leak currents in whole-cell recordings

This paper was submitted directly (Track II) to the PNAS office.

Abbreviations: AMPA, α-amino-3-5-methyl-4-isoxazolepropionic acid; AMPAR, AMPA receptor; I_{pCa}, presynaptic Ca^{2+} currents; I_{pBa}, presynaptic Ba^{2+} currents; I_{pK}, presynaptic K^+ currents; EPSC, excitatory postsynaptic current; MNTB, medial nucleus of the trapezoid body; CTZ, cyclothiazide; D-AP5, D-(-)-2-amino-5-phosphonopentanic acid; aCSF, artificial cerebrospinal fluid; CNQX, 6-cyano-7-nitroquinoxaline-2,3-dione; CPPG, (*R,S*)-α-cyclopropyl-4-phosphonophenylglycine; GluR, glutamate receptor; mGluR, metabotropic GluR.

‡H.T. and Y.N. contributed equally to this work.

§To whom correspondence should be addressed. E-mail: ttakahas-tky@umin.ac.jp.

www.pnas.org/cgi/doi/10.1073/pnas.0408514102

were subtracted by the scaled pulse (P/8) protocol. Current and voltage recordings were made by using a patch-clamp amplifier (Axopatch-1D or Axopatch-200B, Axon Instruments, Union City, CA). Records were low-pass-filtered at 5 kHz and digitized at 20–50 kHz by an analog-digital converter (Digidata 1322A) with PCLAMP8 software (both from Axon Instruments). The liquid-junction potentials between the pipette solutions and aCSF were +2 mV for I_{pCa} and I_{pBa} recordings and +10 mV for I_{pK} recordings, which were not corrected for. Drugs were bath-applied by switching superfusates, using solenoid valves (perfusion rate = 1.5–2.0 ml/min). Experiments were carried out at room temperature (22–25°C). Values in the text and figures are given as mean ± SEM, and statistical comparisons were made by using Student's paired *t* test, unless otherwise noted.

Drugs. Domoate, L-glutamate, guanosine 5′-*O*-(3-thiotriphosphate) (GTPγS), guanosine 5′-*O*-(2-thiodiphosphate) (GDPβS), yohimbine, 8-cyclopentyl-1,3-dimethylxanthine, *N*-(piperidin-1-yl)-5-(4-iodophenyl)-1-(2,4-dichlorophenyl)-4-methyl-1H-pyrazole-3-carboxamide (AM251), *N*ω-nitro-L-arginine, and 2,4′dibromoacetophenone were purchased from Sigma. D-(-)-2-amino-5-phosphonopentanic acid (D-AP5), (*S*)-α-amino-3–5-methyl-4-isoxazolepropionic acid (AMPA), cyclothiazide (CTZ), 6-cyano-7-nitroquinoxaline-2,3-dione (CNQX), (*R*,*S*)-α-cyclopropyl-4-phosphonophenylglycine (CPPG), (*R*,*S*)-α-methyl-4-carboxyphenylglycine, 4-(8-methyl-9H-1,3-dioxolo[4,5-h][2,3]benzodiazepin-5-yl)-benzenamine hydrochloride (GYKI52466), 3-aminopropyl(diethoxymethyl)-phosphinic acid (CGP35348), and (2*S*,4*R*)-4-methylglutamic acid (SYM2081) were purchased from Tocris Cookson (Bristol, U.K.).

Results

An AMPA/Kainate Receptor Agonist Inhibited NMDA-EPSCs. Bath application of the AMPA/kainate receptor agonist domoate (10 μM) inhibited EPSCs recorded at a holding potential of +40 mV at the calyx of Held (Fig. 1*A*). To assess the site of its action, before domoate application, we separated the NMDA receptor and AMPAR components by blocking the former with D-AP5 (50 μM) (Fig. 1*A*, traces a − b and c − d). This treatment revealed that AMPA component returns to the baseline at the peak of NMDA-EPSCs (arrow in trace a). The magnitude of domoate-induced inhibition of NMDA-EPSCs, estimated by subtraction (Fig. 1*A*, trace a − b vs. trace c − d), was 71.8 ± 2.9%, whereas that of AMPA-EPSCs estimated in the presence of D-AP5 (Fig. 1*A*, trace b vs. trace d) was 93.0 ± 1.0% ($n = 4$). Thus, domoate inhibited both AMPA- and NMDA-EPSCs, suggesting that the main site of its action is presynaptic. To confirm the presynaptic site of domoate action, we compared the paired-pulse ratios (PPRs) of EPSCs (interstimulus interval = 20 ms) before and during domoate applications. As shown in Fig. 1*B*, domoate increased PPRs by 102 ± 38% ($n = 7$; $P < 0.05$), confirming that the main site of domoate action is presynaptic. Greater inhibition of AMPA-EPSCs compared with NMDA-EPSCs (Fig. 1*A*) suggests that domoate might additionally affect postsynaptic AMPARs.

Presence of Functional AMPARs at the Calyceal Nerve Terminal. The presynaptic inhibitory effect of domoate on EPSCs implies that functional AMPA/kainate receptors might be expressed in the nerve terminal. We investigated this possibility by making whole-cell recordings directly from calyceal nerve terminals. Bath application of domoate (10 μM) depolarized the terminal by 8.6 ± 0.5 mV ($n = 5$) in current-clamp mode and induced an inward current of 117 ± 20 pA ($n = 6$) under voltage-clamp at a holding potential of −80 mV (Fig. 2*A*). AMPA (10 μM) also depolarized the terminal by 1.7 ± 0.5 mV ($n = 5$; $P < 0.05$) and induced an inward current of 23.5 ± 4.6 pA ($n = 5$; Fig. 2*B*). In the presence of CTZ (100 μM), which blocks AMPAR desensitization, AMPA (10 μM) depolarized the terminal by 7.6 ± 0.6 mV and induced inward currents of 69.2 ± 18.9 pA ($n = 5$; Fig. 2*C*). AMPA/kainate receptor antagonist CNQX (20 μM) abolished these effects ($n = 4$; Fig. 2*D*). These results indicate that the calyx of Held terminal

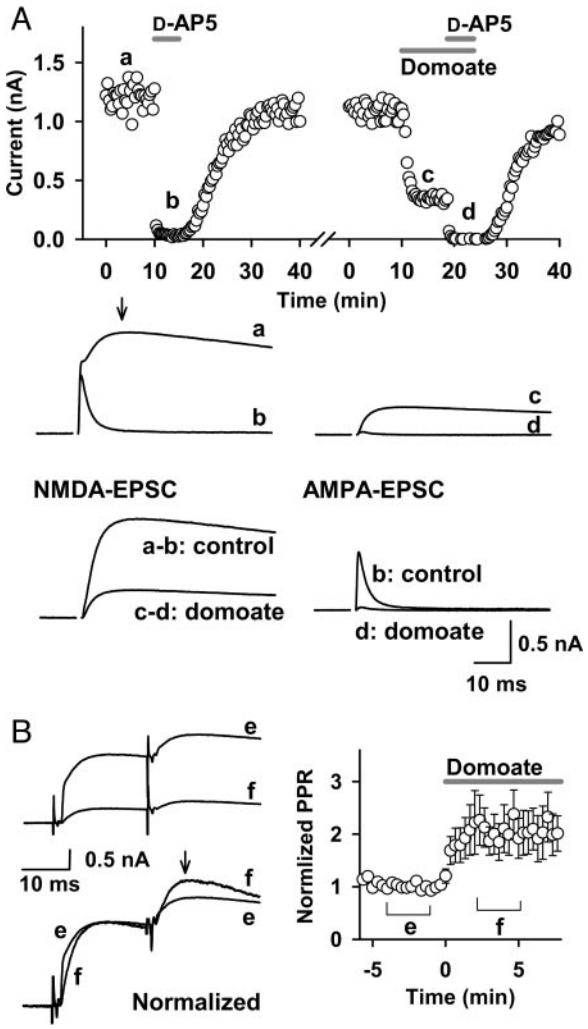

Fig. 1. The AMPA/kainate receptor agonist domoate presynaptically attenuates EPSCs. (*A*) Amplitudes of NMDA-EPSCs (ordinate) deduced from the peak amplitude of a slow component of EPSCs (at 10–15 ms from the onset, arrow in trace a) evoked at a holding potential of +40 mV. D-AP5 (50 μM) abolished this component (trace b). Domoate (10 μM) attenuated EPSCs (trace c). D-AP5 abolished the remaining component in the presence of domoate (trace d). Sample traces show NMDA components and AMPA components of EPSCs, the former being obtained by subtracting the D-AP5-resitant (AMPA) component before (a and b) and during (c and d) domoate application (superimposed). Both NMDA (a − b) and AMPA (b) components of EPSCs were attenuated by domoate (c − d and d). Input resistance of MNTB neurons was 29.8 ± 3.2 MΩ and 23.4 ± 1.9 MΩ (at +40 mV, $n = 4$) before and during domoate application, respectively. (*B*) EPSCs evoked by the paired-pulse stimulation (interpulse interval, 20 ms) at +40 mV before and during domoate application (superimposed in traces). (*Left*) EPSCs before (trace e) and during (trace f) domoate applications are superimposed with (*Lower*) or without (*Upper*) normalization at the first amplitude. Slowing in the rise time of EPSCs during domoate application (first EPSCs in the normalized and superimposed trace) is consistent with the stronger inhibitory effect of domoate on AMPA-EPSCs. (*Right*) Time plot of paired-pulse ratios (PPRs) normalized to the control value (mean of 10 points before domoate application). The arrow indicates the point at which the second EPSC amplitude was measured. Data points and error bars during domoate application (bar) indicate mean values and SEMs of PPRs relative to control.

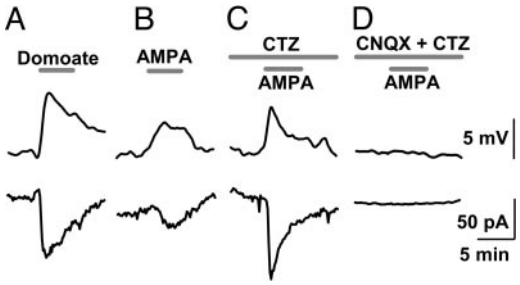

Fig. 2. Effects of AMPA/kainate receptor agonists on membrane potential and membrane currents of the calyceal nerve terminal. Depolarization (*Upper*) and inward currents (*Lower*) induced by domoate (10 μM) (*A*), AMPA (10 μM) (*B*), and AMPA (10 μM) with CTZ (100 μM) (*C* and *D*) in the absence (*C*) or presence (*D*) of CNQX (20 μM). CNQX abolished the inward currents ($n = 4$) and depolarization ($n = 4$) induced by AMPA with CTZ. Resting membrane potential of the nerve terminal was -67.1 ± 2.0 mV ($n = 19$).

expresses functional AMPARs, which are more strongly desensitized by AMPA than by domoate, as previously reported in somatic glutamate receptors (GluRs) (13).

AMPA Receptor Agonists Inhibit Presynaptic Ca^{2+} Currents but Do Not Affect K^+ Currents. At the calyx of Held, presynaptic depolarization up to 10 mV moderately potentiates EPSCs (14, 15). Therefore, the presynaptic inhibitory effect of domoate (Fig. 1) cannot be explained by the direct depolarizing effect of AMPAR agonists on the terminal (Fig. 2). Thus, we examined the possibility that AMPAR agonists might affect I_{pCa} by means of a metabotropic pathway. As illustrated in Fig. 3*A1*, bath application of domoate (10 μM) attenuated I_{pCa} in a reversible manner by $12.1 \pm 2.0\%$ (at 0 mV, $n = 6$; $P < 0.01$; Fig. 3*A2*). The selective AMPAR antagonist 4-(8-methyl-9H-1,3-dioxolo[4,5-h][2,3]benzodiazepin-5-yl)-benzenamine hydrochloride (GYKI52466) (100 μM) abolished this effect of domoate (Fig. 3*A3*), confirming that it is mediated by AMPARs. Bath application of AMPA (10 μM) alone slightly attenuated I_{pCa} ($2.4 \pm 0.3\%$; $n = 5$; data not shown), and in the presence of CTZ (100 μM), it attenuated I_{pCa} by $18.9 \pm 3.6\%$ (at 0 mV, $n = 5$; $P < 0.01$; Fig. 3*B*). Bath application of the endogenous ligand L-glutamate (100 μM) inhibited I_{pCa} by $33.7 \pm 1.3\%$ ($n = 4$) in the absence of CTZ but in the presence of the metabotropic glutamate receptor (mGluR) antagonists CPPG (300 μM) and (*R,S*)-α-methyl-4-carboxyphenylglycine (500 μM) (Fig. 3*C*). CNQX (20 μM) attenuated this inhibitory effect of L-glutamate by 48% (I_{pCa} inhibition with CNQX $= 16.1 \pm 2.5\%$; $n = 4$), suggesting that L-glutamate activated presynaptic AMPARs, thereby inhibiting I_{pCa}. The CNQX-resistant I_{pCa} inhibition by L-glutamate might arise from mGluRs resistant to the antagonists used.

We next investigated whether AMPAR agonists might affect I_{pK} (17). As shown in Fig. 3*D*, domoate (10 μM) had no effect on I_{pK} at all voltages examined. Similarly, AMPA with CTZ had no effect on I_{pK} ($n = 5$; see Fig. 6, which is published as supporting information on the PNAS web site).

G Proteins Are Involved in the AMPAR-Mediated Inhibition of I_{pCa}. We next examined whether G proteins might mediate the inhibitory effect of AMPAR agonists (3, 8, 18) by loading the nonhydrolyzable GTP analogue GTPγS (0.2 mM) into the calyceal terminal by means of presynaptic patch pipettes. In the presence of GTPγS, AMPA (+CTZ) no longer inhibited I_{pCa} ($n = 5$; Fig.

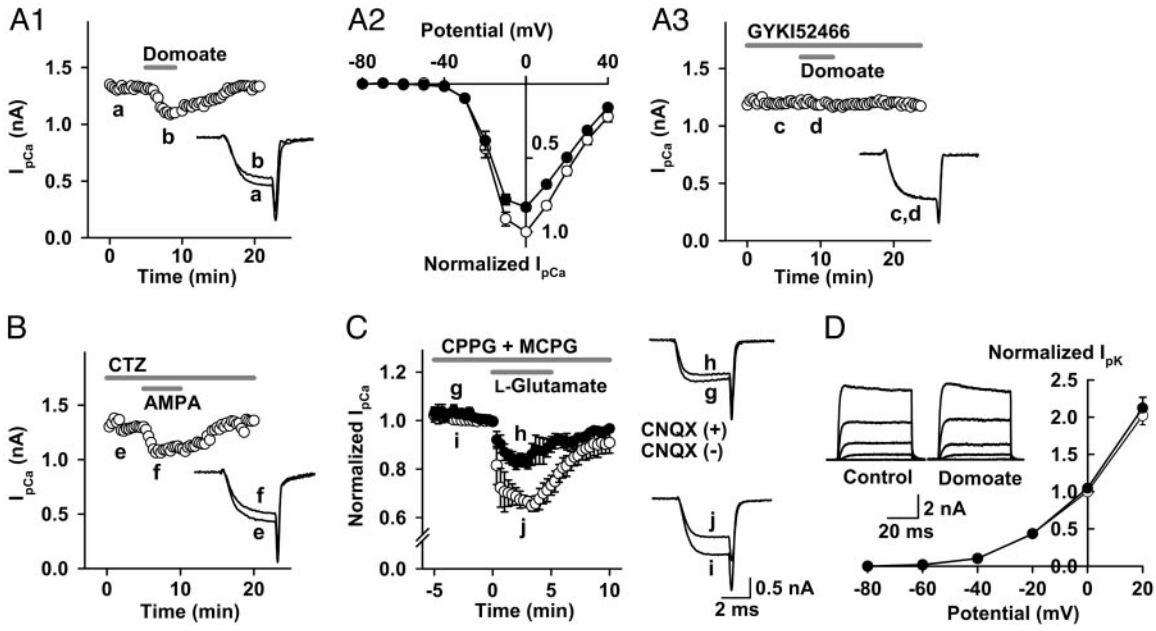

Fig. 3. AMPA receptor agonists inhibit presynaptic Ca^{2+} currents without affecting K^+ currents. (*A–C*) I_{pCa} was evoked by a 3.8-ms depolarizing pulse to 0 mV here and in Figs. 4*A* and 5 *A* and *B*. (*A*) Domoate inhibited I_{pCa}. (*A1*) Time plot and sample traces of I_{pCa} before (trace a) and during (trace b) application of domoate (10 μM, superimposed). (*A2*) The current-voltage relationships of I_{pCa} before (open circles) and during (filled circles) application of domoate. Data are derived from four calyces. The current amplitude was normalized to the control value at 0 mV here and in Figs. 3*D* and 4*B*. (*A3*) The AMPAR antagonist 4-(8-methyl-9H-1,3-dioxolo[4,5-h][2,3]benzodiazepin-5-yl)-benzenamine hydrochloride (GYKI52466) (100 μM) blocked the effect of domoate on I_{pCa} ($0.2 \pm 0.1\%$; $n = 5$ for sample traces c and d). (*B*) AMPA inhibited I_{pCa} in the presence of CTZ (100 μM). Because CTZ by itself slightly attenuates I_{pCa} (16), it was applied 10 min before testing AMPA. (*C*) L-glutamate inhibited I_{pCa}. In the presence of CPPG (300 μM) and (*R,S*)-α-methyl-4-carboxyphenylglycine (500 μM), L-glutamate (100 μM) inhibited I_{pCa} (open circles, superimposed traces i and j), and this effect was partially attenuated by CNQX (20 μM, filled circles, traces g and h). (*D*) Domoate (10 μM) had no effect on I_{pK} evoked by a 50-ms depolarizing pulse stepping to various potentials (averaged I_{pK} at each potential are superimposed in traces). In the current-voltage relationships, the mean amplitude of I_{pK} was normalized to control at 0 mV. Open and filled circles represent data points before and during application of domoate ($n = 5$).

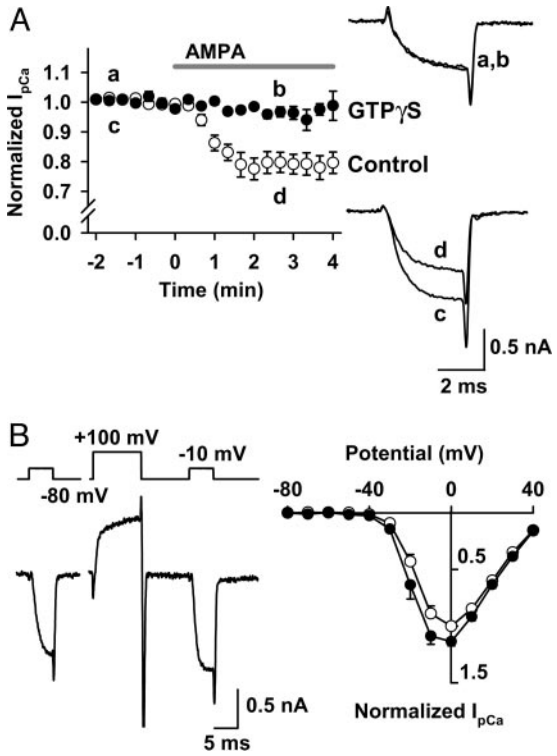

Fig. 4. AMPAR-dependent I_{pCa} inhibition involves heterotrimeric G proteins. I_{pCa} was evoked by a depolarizing test pulse stepping to 0 mV. CTZ (100 μM) was present throughout. (*A*) GTPγS (0.2 mM) loaded into the presynaptic terminal from the patch pipette blocked the AMPA-induced I_{pCa} inhibition. Sample records are averaged I_{pCa} before (traces a and c) and during (traces b and d) application of AMPA, with (a and b) or without (c and d) GTPγS. Data points and bars indicate mean ± SEM (n = 5 each). (*B*) Voltage-dependent disinhibition of I_{pCa}. In the presence of AMPA (10 μM), I_{pCa} was evoked by pulses (5 ms) stepping to various potentials before and 10 ms after a conditioning pulse stepping to +100 mV for 10 ms. (*Left*) Command voltage protocol (*Upper*) and I_{pCa} (*Lower*). (*Right*) Current-voltage relationships of I_{pCa} before (filled circles) and after (open circles) the conditioning pulse. Data are derived from five calyces.

4*A*). Intraterminal loading of the GDP analogue GDPβS (3 mM) also significantly attenuated the AMPA-induced I_{pCa} inhibition (from 18.9 ± 3.6% to 9.6 ± 1.0%; n = 5; $P < 0.02$, unpaired t test). These results indicate that G proteins are involved in the presynaptic inhibitory effect of AMPAR agonists on I_{pCa}.

Inhibition of calcium currents mediated by the G protein $\beta\gamma$-subunit (G$\beta\gamma$) can be removed by a strong depolarizing prepulse, which transforms the voltage gates of Ca^{2+} channels from a reluctant state to a willing state (19–21). We examined whether this voltage-dependent unblock might be observed for the AMPA-induced I_{pCa} inhibition. As shown in Fig. 4*B*, a conditioning prepulse (from −80 mV to +100 mV for 10 ms) significantly disinhibited I_{pCa} evoked by the test pulses (5 ms to different membrane potentials; $P < 0.05$ at −20, −10, and 0 mV; n = 5), suggesting that the AMPA-induced I_{pCa} inhibition may be mediated by G$\beta\gamma$.

Direct Inhibitory Effect of AMPA on I_{pCa}. Our present results suggest that AMPAR agonists directly activate presynaptic AMPARs and inhibit I_{pCa} by means of G proteins. However, it might be argued that the inhibitory effect of AMPAR agonists arose secondarily from their actions on AMPARs in surrounding cells in slices. Given that tetrodotoxin is present in the aCSF, depolarization of somata by AMPAR activation is unlikely to depolarize nerve terminals. However, local depolarization of nerve terminals or somata by means of AMPAR activation might release transmitters and/or neuromodulators such as GABA, glutamate, adenosine, and noradrenaline, thereby indirectly activating G protein-coupled receptors (GPCRs) in the calyceal presynaptic terminal (22–25). To examine this possibility, we first tested the effect of AMPA (with CTZ) on I_{pCa} in the presence of GPCR antagonists, including the $GABA_B$ receptor antagonist 3-aminopropyl(diethoxymethyl)phosphinic acid (CGP35348) (100 μM), the group II/III mGluR antagonist CPPG (300 μM), the adrenaline α_2 receptor antagonist yohimbine (20 μM), and the adenosine A_1 receptor antagonist 8-cyclopentyl-1,3-dimethylxanthine (10 μM) (Fig. 5*A*). We also added the kainate receptor-desensitizing antagonist (2*S*,4*R*)-4-methylglutamic acid (SYM2081) (3 μM) to examine whether kainite receptors are involved. In this solution, AMPA (10 μM with CTZ) inhibited I_{pCa} by 23.7 ± 2.6% (n = 5 at 0 mV; Fig. 5A), which was similar to the inhibition without the antagonists (P = 0.32, unpaired t test). Thus, these results pharmacologically rule out the involvement of $GABA_B$ receptors, mGluRs, α_2 receptors, A_1 receptors, and kainate receptors in the AMPA-induced I_{pCa} inhibition. However, these results do not entirely rule out the possible involvement of as yet unidentified messengers, which might be released in response to AMPAR agonists. To examine this possibility, we made two types of experiments. First, we destroyed postsynaptic MNTB cells by gentle blows and suctions of cell membrane through a largish patch pipette (orifice diameter ≈ 3–5 μm). After destroying the postsynaptic cells, calyceal terminals were practically isolated from surrounding cells (Fig. 5*B*). Bath application of AMPA (10 μM plus 100 μM CTZ) to these calyces clearly inhibited I_{pCa} by 18.9 ± 3.0% (at 0 mV, n = 5), which is similar in magnitude to control. Second, we blocked depolarization-induced exocytosis by replacing Ca^{2+} in the aCSF with Ba^{2+}, which nearly abolished synaptic transmission at the calyx of Held (Fig. 7*A*, which is published as supporting information on the PNAS web site) as previously reported at the squid giant synapse (26) and also markedly attenuated the potassium-induced increase in the miniature EPSC frequency (Fig. 7*B*). Furthermore, to exclude possible involvements of retrograde messengers, we included 4-methyl-1H-pyrazole-3-carboxamide (AM251) (5 μM), *N*ω-nitro-L-arginine (1 mM), and 2,4′dibromoacetophenone (10 μM) in the aCSF to block cannabinoid CB1 receptors (27), NO synthetase, and phospholipase A_2, respectively. Even in this condition, AMPA (10 μM plus CTZ) inhibited I_{pBa} by 18.8 ± 2.9% (n = 5; Fig. 5*C*) to a similar extent as it inhibited I_{pCa} (Fig. 3*B*). Furthermore, GTPγS (0.2 mM) loaded into the calyceal terminals abolished the inhibitory effect of AMPA on I_{pBa} (0.8 ± 0.7%; n = 5). Taken together, these results strongly suggest that direct activation of functional AMPARs in the calyceal terminal inhibits presynaptic Ca^{2+} currents by means of G proteins.

Discussion

By taking advantage of the large calyx of Held nerve terminal, we have demonstrated that activation of presynaptic AMPARs inhibits voltage-gated Ca^{2+} channels by means of G proteins, most likely through G$\beta\gamma$, thereby inhibiting transmitter release from the nerve terminal. Presynaptic AMPARs also showed an ionotropic nature, depolarizing the nerve terminal by 5–10 mV upon activation by ligands. Although presynaptic depolarization of this magnitude increases transmitter release (14, 15), this facilitatory effect seems to be masked by the stronger inhibitory effect mediated by G proteins.

Biochemical studies first demonstrated that activation of AMPARs inhibits adenylyl cyclase by means of Gi (3). Subsequently, in retinal ganglion cells, activation of AMPARs was shown to inhibit cGMP-gated currents in a G protein-dependent manner (18). More recently, at a cerebellar inhibitory synapse, the G protein inhibitor *N*-ethylmaleimide is reported to attenuate the AMPAR-mediated

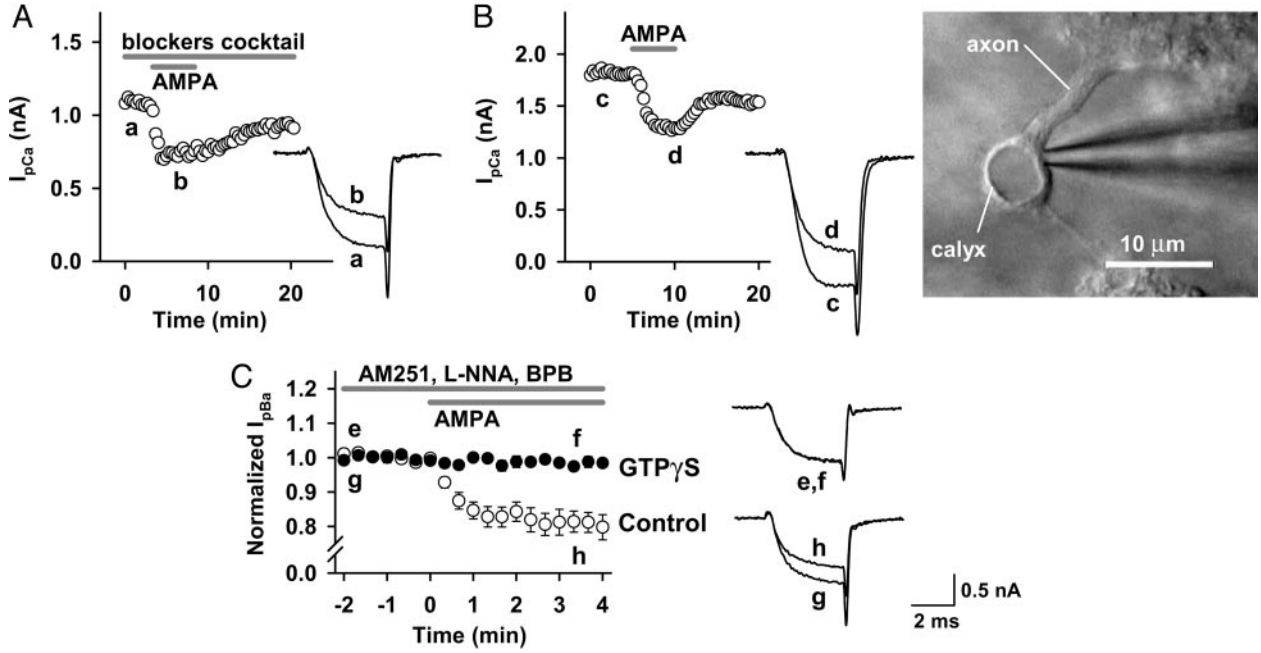

Fig. 5. Direct inhibitory effect of AMPA on presynaptic Ca^{2+} channel currents. CTZ (100 μM) was present throughout. (*A*) AMPA (10 μM) inhibited I_{pCa} in the presence of 3-aminopropyl(diethoxymethyl)phosphinic acid (CGP35348) (100 μM), CPPG (300 μM), 8-cyclopentyl-1,3-dimethylxanthine (10 μM), yohimbine (20 μM), and (2*S*,4*R*)-4-methylglutamic acid (SYM2081) (3 μM), which had been applied 10 min before application of AMPA. (*B*) AMPA (10 μM) inhibited I_{pCa} recorded from calyceal terminals after destroying postsynaptic cells. (*Right*) An isolated calyceal terminal attached with a patch pipette. (*C*) Inhibition of I_{pBa} by AMPA (10 μM, open circles in time plots, superimposed traces f and g) after blocking synaptic transmission by replacing external Ca^{2+} with Ba^{2+} (see Fig. 7). The aCSF contained the retrograde messenger blockers 4-methyl-1H-pyrazole-3-carboxamide (AM251) (5 μM), *N*ω-nitro-L-arginine (1 mM), and 2,4′dibromoacetophenone (10 μM). Intraterminal free Ca^{2+} concentration was set at 90 nM with a Ca^{2+} buffer (6 mM $CaCl_2$/10 mM EGTA) included in the patch pipette to preserve the G protein-mediated inhibition of Ba^{2+} currents (28). In the absence of Ca^{2+} in the pipette solution, the I_{pBa} inhibition by AMPA (10 μM) was smaller (6.0 $\pm$ 1.7%; $n = 5$; data not shown). When GTPγS (0.2 mM) was included in the pipette solution (together with 90 nM Ca^{2+} buffer), AMPA (10 μM) no longer inhibited Ba^{2+} currents (filled circles). Data are derived from five terminals each for control and GTPγS loading. Sample records are I_{pBa} in the presence (traces e and f, superimposed) and absence (traces g and h, superimposed) of GTPγS before (e and g) and during (f and h) application of AMPA (10 μM).

presynaptic inhibition (8). Our present results are in line with these reports and demonstrate more directly that AMPARs are coupled with heterotrimeric G proteins in the nerve terminal and that their activation leads to inhibition of voltage-gated Ca^{2+} channels. The detailed molecular mechanism by which AMPARs couple with G proteins remains to be determined.

Ionotropic GluRs comprise three categories: AMPARs, NMDA receptors (NMDARs), and kainate receptors (1, 2), all of which are expressed in nerve terminals, in addition to postsynaptic neurons. NMDARs are expressed in cerebellar nerve terminals (29) and are involved in the long-term depression of excitatory transmission (30) or the retrograde enhancement of transmitter release (31). NMDARs are also expressed at the primary afferent terminals in the spinal cord (32) and are thought to regulate action potential invasion (33). However, it is not known whether presynaptic NMDARs are linked with G proteins. Kainate receptors expressed in hippocampal nerve terminals modulate transmitter release (34–36) bidirectionally, depending on the concentration of the agonist (37). Kainate receptors expressed in dorsal root ganglion cells are coupled with G proteins and inhibit Ca^{2+} channels upon activation with agonists (38). In the hippocampus, both at the inhibitory (39, 40) and excitatory (41) synapses, presynaptic kainate receptors are proposed to couple with G proteins for inhibiting transmitter release. Although we did not observe kainate receptor-dependent presynaptic inhibition at the calyx of Held terminal, a common intracellular mechanism might underlie the presynaptic inhibition by kainate receptors and AMPA receptors.

It has been reported that the glutamate receptor (GluR) subunits of AMPARs are expressed at various nerve terminals. Axonal growth cones of hippocampal neurons are immunopositive to GluR1 and GluR2 (42). Similarly, GluR1–4 immunoreactivities are observed at the nerve terminal of developing rat striatum (5) and at the primary afferent terminals (6). GluR4 immunogold particles are observed in presynaptic structures at the hair cell ribbon synapse (43) and at the end bulb of Held synapse in the anteroventral cochlear nucleus of auditory brainstem (44). At cerebellar inhibitory synapses (8, 45) and spinal cord excitatory synapses (7), presynaptic AMPARs inhibit transmitter release. Thus, the AMPAR-mediated presynaptic inhibition may be widespread among central synapses.

At the excitatory synapse, glutamate released from nerve terminals can inhibit transmitter release by means of activating mGluRs and AMPA/kainate receptors in the nerve terminal, both of which inhibit presynaptic Ca^{2+} entry by means of G protein activation. In this respect, metabotropic and ionotropic glutamate autoreceptors may cooperate for saving transmitters from depletion and protecting neurons from glutamate excitotoxicity in the pathological conditions. Although bath application of L-glutamate inhibited presynaptic Ca^{2+} currents by means of AMPAR activation, we could not detect inhibition of presynaptic Ca^{2+} currents by glutamate released by repetitive presynaptic stimulation (10–200 Hz; $n = 5$; data not shown). However, this result does not preclude physiological or pathological roles of presynaptic AMPARs at the calyx of Held *in vivo*. More importantly, our results suggest that presynaptic AMPARs at various central synapses may play a regulatory role for transmitter release by means of heterotrimeric G proteins.

We thank Mark Farrant, Shiro Konishi, and Tetsuhiro Tsujimoto for comments on the manuscript and Ken Kitamura for advice. This work was supported by a Grant-in-Aid for Specially Promoted Research from the Ministry of Education, Culture, Sports, Science, and Technology.

1. Nakanishi, S. (1992) *Science* **258,** 597–603.
2. Hollmann, M. & Heinemann, S. (1994) *Annu. Rev. Neurosci.* **17,** 31–108.
3. Wang, Y., Small, D. L., Stanimirovic, D. B., Morley, P. & Durkin, J. P. (1997) *Nature* **389,** 502–504.
4. Hayashi, T., Umemori, H., Mishina, M. & Yamamoto, T. (1999) *Nature* **397,** 72–76.
5. Fabian-Fine, R., Volknandt, W., Fine, A. & Stewart, M. G. (2000) *Eur. J. Neurosci.* **12,** 3687–3700.
6. Lu, C. R., Hwang, S. J., Phend, K. D., Rustioni, A. & Valtschanoff, J. G. (2002) *J. Neurosci.* **22,** 9522–9529.
7. Lee, C. J., Bardoni, R., Tong, C. K., Engelman, H. S., Joseph, D. J., Magherini, P. C. & MacDermott, A. B. (2002) *Neuron* **35,** 135–146.
8. Satake, S., Saitow, F., Rusakov, D. & Konishi, S. (2004) *Eur. J. Neurosci.* **19,** 2464–2474.
9. Forsythe, I. D. (1994) *J. Physiol.* **479,** 381–387.
10. Hori, T., Takai, Y. & Takahashi, T. (1999) *J. Neurosci.* **19,** 7262–7267.
11. Takahashi, T., Hori, T., Kajikawa, Y. & Tsujimoto, T. (2000) *Science* **289,** 460–463.
12. Forsythe, I. D. & Barnes-Davies, M. (1993) *Proc. R. Soc. London Ser. B* **251,** 151–157.
13. Mayer, M. & Vyklicky, L., Jr. (1989) *Proc. Natl. Acad. Sci. USA* **86,** 1411–1415.
14. Turecek, R. & Trussell, L. O. (2001) *Nature* **411,** 587–590.
15. Kaneko, M. & Takahashi, T. (2004) *J. Neurosci.* **24,** 5202–5208.
16. Ishikawa, T. & Takahashi, T. (2001) *J. Physiol.* **533,** 423–431.
17. Ishikawa, T., Nakamura, Y., Saitoh, N., Li, W. B., Iwasaki, S. & Takahashi, T. (2003) *J. Neurosci.* **23,** 10445–10453.
18. Kawai, F. & Sterling, P. (1999) *J. Neurosci.* **19,** 2954–2959.
19. Ikeda, S. R. (1991) *J. Physiol.* **439,** 181–214.
20. Kasai, H. (1992) *J. Physiol.* **448,** 189–209.
21. Kajikawa, Y., Saitoh, N. & Takahashi, T. (2001) *Proc. Natl. Acad. Sci. USA* **98,** 8054–8058.
22. Takahashi, T., Forsythe, I. D., Tsujimoto, T., Barnes-Davies, M. & Onodera, K. (1996) *Science* **274,** 594–597.
23. Takahashi, T., Kajikawa, Y. & Tsujimoto, T. (1998) *J. Neurosci.* **18,** 3138–3146.
24. Leao, R. M. & von Gersdorff, H. (2002) *J. Neurophysiol.* **87,** 2297–2306.
25. Kimura, M., Saitoh, N. & Takahashi, T. (2003) *J. Physiol.* **553,** 415–426.
26. Augustine, G. J. & Eckert, R. (1984) *J. Physiol.* **346,** 257–271.
27. Kushmerick, C., Price, G. D., Taschenberger, H., Puente, N., Renden, R., Wadiche, J. I., Duvoisin, R. M., Grandes, P. & von Gersdorff, H. (2004) *J. Neurosci.* **24,** 5955–5965.
28. Lester, R. A. & Jahr, C. E. (1990) *Neuron* **4,** 741–749.
29. Casado, M., Dieudonne, S. & Ascher, P. (2000) *Proc. Natl. Acad. Sci. USA* **97,** 11593–11597.
30. Casado, M., Isope, P. & Ascher, P. (2002) *Neuron* **33,** 123–130.
31. Duguid, I. C. & Smart, T. G. (2004) *Nat. Neurosci.* **7,** 525–533.
32. Lu, C. R., Hwang, S. J., Phend, K. D., Rustioni, A. & Valtschanoff, J. G. (2003) *J. Comp. Neurol.* **460,** 191–202.
33. Bardoni, R., Torsney, C., Tong, C. K., Prandini, M. & MacDermott, A. B. (2004) *J. Neurosci.* **24,** 2774–2781.
34. Chittajallu, R., Vignes, M., Dev, K. K., Barnes, J. M., Collingridge, G. L. & Henley, J. M. (1996) *Nature* **379,** 78–81.
35. Kamiya, H. & Ozawa, S. (2000) *J. Physiol.* **523,** 653–665.
36. Schmitz, D., Frerking, M. & Nicoll, R. A. (2000) *Neuron* **27,** 327–338.
37. Schmitz, D., Mellor, J. & Nicoll, R. A. (2001) *Science* **291,** 1972–1976.
38. Rozas, J. L., Paternain, A. V. & Lerma, J. (2003) *Neuron* **39**, 543–553.
39. Rodríguez -Moreno, A. & Lerma, J. (1998) *Neuron* **20,** 1211–1218.
40. Rodríguez-Moreno, A., López-García, J. C. & Lerma, J. (2000) *Proc. Natl. Acad. Sci. USA* **97,** 1293–1298.
41. Frerking, M., Schmitz, D., Zhou, Q., Johansen, J. & Nicoll, R. A. (2001) *J. Neurosci.* **21,** 2958–2966.
42. Schenk, U., Verderio, C., Benfenati, F. & Matteoli, M. (2003) *EMBO J.* **22,** 558–568.
43. Matsubara, A., Laake, J. H., Davanger, D., Usami, S. & Ottersen, O. P. (1996) *J. Neurosci.* **16,** 4457–4467.
44. Wang, Y.-X., Wenthold, R. J., Ottersen, O. P. & Petralia, R. S. (1998) *J. Neurosci.* **18,** 1148–1160.
45. Satake, S., Saitow, F., Yamada, J. & Konishi, S. (2000) *Nat. Neurosci.* **3,** 551–558.